Structural Engineering and Mechanics, Vol. 7, No. 4 (1999) 361-375
DOI: http://dx.doi.org/10.12989/sem.1999.7.4.361

Out-of-plane vibration of multi-span curved beam due to moving loads

Rong-Tyai Wang† and Yiu-Lo Sang‡

Department of Engineering Science, National Cheng Kung University, Taiwan, R.O.C.

Abstract. This paper presents an analytic method of examining the out-of-plane vibration of continuous curved beam on periodical supports. The orthogonality of two distinct sets of mode shape functions is derived. The forced vibration of beam due to moving loads is examined. Two types of moving loads, which are concentrated load and uniformly distributed load, are considered. The response characteristics of beam induced by these loads are investigated as well.

Key words: out-of-plane; curved beam; orthogonality; moving loads.

1. Introduction

The out-of-plane vibration of curved beams is broadly encountered in engineering. The curved guideway is similar to a multi-span curved beam. Loads moving on a curved beam induce the transverse deflection, bending slope and twist angle of the structure. The responses of a curved beam owing to moving loads are very different from those of the same beam due to static loads. However, the problem of loads moving on the curved beam has never been investigated. The velocity of moving vehicles on curved guideways is more rapid than previously. Consequently, this topic continues to be an interesting topic in structural dynamics in recent years. Volterra and Gaines (1971) presented the static equation of out-of-plane equilibrium of curved Bernoulli-Euler beams. Rao (1971) neglected the warping effect and included the effects of rotatory inertia and transverse shear deformation to derive the equations of motion of curved beam. Wang *et al.* (1980) adopted Rao's equations to calculate modal frequencies of continuous curved Bernoulli-Euler beam. The Bernoulli-Euler beam theory is suitable only for examining the flexural vibration of a slender beam within a low frequency range. The phase wave velocity predicated from the Bernoulli-Euler beam theory is unreasonable within a higher frequency. The response of either a beam with a larger ratio of radius of gyration of cross-sectional area to length or higher modes can be only obtained well by the Timoshenko beam theory. According to this reason, Wang *et al.* (1984) extended Rao's equations again to set up a dynamic stiffness matrix for determining the modal frequencies of a continuously curved Timoshenko beam. Silva *et al.* (1988) also adopted Rao's equations to study the dynamic response of a continuously curved Timoshenko beam.

The finite element technique is normally adopted to examine a curved beam subjected to a static load (Lebeck 1985 and El-Amin 1978) or the problem of buckling (Yang *et al.* 1986). The

† Professor
‡ Graduate Student

modal frequencies of curved beam determined by the technique have rarely been discussed. Moreover, even the frequencies which can be obtained by the technique are approximate values. The modal frequencies of multi-span curved beam obtained from the method of dynamic stiffness matrix need solving a larger determinant. In addition, the method can not be applied to examine the general vibration of curved beam. These difficulties indicate this method is unfeasible for a multi-span curved beam. Therefore, a more practical way towards studying the out-of-plane vibration of curved beam needs to be investigated.

All the previously cited studies concerning the modal frequencies of curved beams are based on Rao's equations. To examine the out-of-plane vibration of continuously curved beam in the present study, the effects of transverse shear and rotatory inertia of cross section are also included. The curved beam is considered to be compact solid. Therefore, the warping effect is negligible. The curved beam has periodically simple, rigid and non-twisting supports. Furthermore, the width is less than the initial radius of central line. The displacement fields contain bending slope, vertical displacement and twist angle . The strain fields are derived. The stress-strain relations are then set. The stress resultants and stress couples are obtained. The equations of motion similar to Rao's (1971) are then obtained from the Hamilton's principle.

This study presents an analytic method to obtain the frequency responses of each span. The transfer matrix of responses of each span is then established for determining the modal frequencies and their corresponding sets of mode shape functions of the complete beam. Effects of initial radius of central line, subtend angle of each span and span number on the modal frequencies are investigated. The orthogonality of any two distinct sets of mode shape functions is demonstrated. The method of modal analysis is then outlined to study the vibration of beam induced by moving loads. A concentrated load and a uniformly distributed load are considered herein. The response characteristics of beam owing to these loads will be investigated.

2. Equations of motion

A continuously curved beam resting on periodically n+1 hinge supports is depicted in Fig. 1. These supports are rigid and non-twisting. The radius of curved beam is R. The angle measured from the bisector of angle between any two adjacent supports is α. A distributed load $f(\theta, t)$ on the n-span curved beam is illustrated in Fig. 2. The beam is homogeneous and isotropic with mass density ρ, Young's modulus E, shear modulus G, shear coefficient κ and Poisson's ratio μ. The Cartesian coordinates x, y and z system and the cylindrical coordinates r, θ and z system for a typical span are depicted in Fig. 3(a). The x and the z axes coincide with the principal centroidal axes of the beam, while the y axis is tangent to the curved axis of the beam. The coordinates r, θ

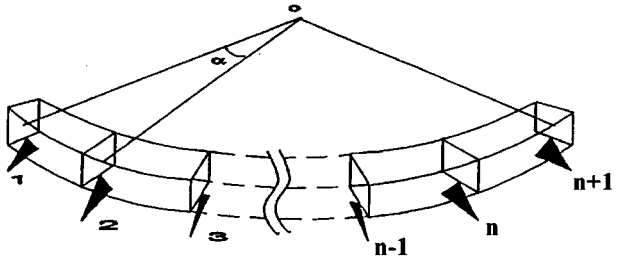

Fig. 1 A continuous curved rested on n+1 non-twisting and hinge supports

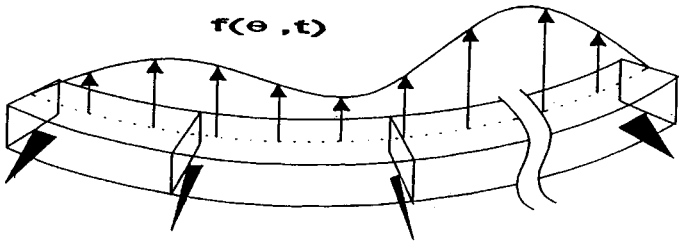

Fig. 2 A distributed load $f(\theta, t)$ on the curved beam

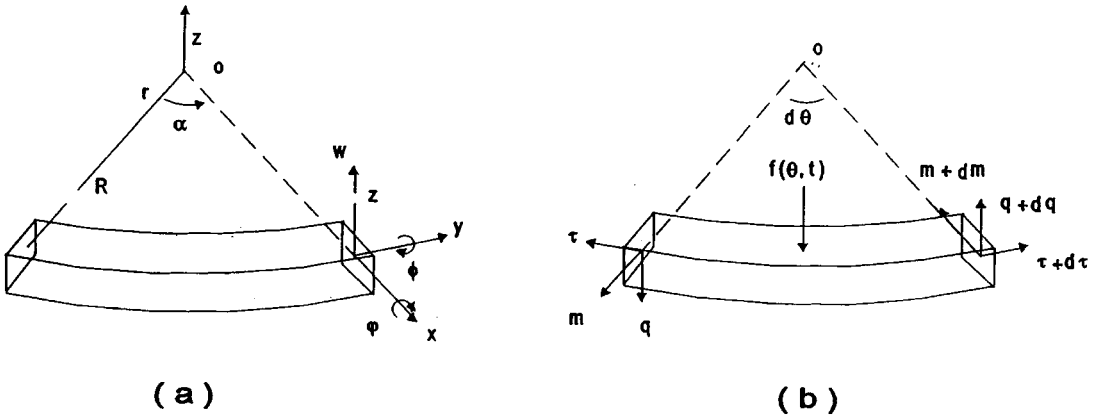

Fig. 3 Geometry, forces and displacements of a typical span of curved beam

and z are taken at the center of curvature of beam. Each span of the beam has width a, thickness h, uniform cross-sectional area A, polar moment J about the y axis, second moment of area I about the direction of the radius. The transverse deflection, bending slope, twist angle of the cross section of beam at the centroidal axes are denoted as w, φ and ϕ, respectively. The width is assumed to be less than the radius of curved beam.

The displacement fields of the cross section along these principal axes in the Cartesian coordinates are

$$u_x = z\phi, \quad u_y = -z\varphi, \quad u_z = w - x\phi \tag{1a}$$

or in the cylindrical coordinates are

$$u_r = z\phi, \quad u_\theta = -z\varphi, \quad u_z = w - (r - R)\phi \tag{1b}$$

The strain components in the cylindrical coordinates are

$$\varepsilon_{rr} = \frac{\partial u_r}{\partial r}, \quad \varepsilon_{\theta\theta} = \frac{1}{r}\frac{\partial u_\theta}{\partial \theta} + \frac{u_r}{r}, \quad \varepsilon_{zz} = \frac{\partial u_z}{\partial z}$$

$$\gamma_{r\theta} = \frac{\partial u_\theta}{\partial r} + \frac{1}{r}\frac{\partial u_r}{\partial \theta} - \frac{u_\theta}{r}, \quad \gamma_{rz} = \frac{\partial u_r}{\partial z} + \frac{\partial u_z}{\partial r}, \quad \gamma_{\theta z} = \frac{\partial u_\theta}{\partial z} + \frac{1}{r}\frac{\partial u_z}{\partial \theta} \tag{2}$$

By using the geometric relations $y=R\theta$ and $r=R+x$, the strain components in the Cartesian coordinates are expressed as

$$\varepsilon_{xx} = \frac{\partial u_x}{\partial x}, \quad \varepsilon_{yy} = \frac{R}{r}\left(\frac{\partial u_y}{\partial y} + \frac{u_x}{R}\right), \quad \varepsilon_{zz} = \frac{\partial u_z}{\partial z}$$

$$\gamma_{xy}=\frac{\partial u_y}{\partial x}+\frac{R}{r}\left(\frac{\partial u_x}{\partial y}-\frac{u_y}{R}\right),\quad \gamma_{zx}=\frac{\partial u_x}{\partial z}+\frac{\partial u_z}{\partial x},\quad \gamma_{yz}=\frac{\partial u_y}{\partial z}+\frac{R}{r}\frac{\partial u_z}{\partial y} \tag{3}$$

Substituting Eq. (1a) into Eq. (3) yields the displacement-strain relations

$$\varepsilon_{xx}=0,\quad \varepsilon_{yy}=\frac{zR}{r}\left(\frac{\phi}{R}-\frac{\partial \varphi}{\partial y}\right),\quad \varepsilon_{zz}=0$$

$$\gamma_{xy}=\frac{zR}{r}\left(\frac{\partial \phi}{\partial y}+\frac{\varphi}{R}\right),\quad \gamma_{zx}=0,\quad \gamma_{yz}=\frac{R}{r}\left(-\frac{r\varphi}{R}+\frac{\partial w}{\partial y}-x\frac{\partial \phi}{\partial y}\right) \tag{4}$$

Employing the relation

$$\frac{R}{r}=\frac{R}{R+x}=\frac{1}{1+\frac{x}{R}}=1-\left(\frac{x}{R}\right)+\left(\frac{x}{R}\right)^2+\cdots$$

into Eq. (4) and neglecting the terms $O(x/R)$ yield the strain components

$$\varepsilon_{xx}=0,\quad \varepsilon_{yy}=z\left(\frac{\phi}{R}-\frac{\partial \varphi}{\partial y}\right),\quad \varepsilon_{zz}=0,$$

$$\gamma_{xy}=z\left(\frac{\partial \phi}{\partial y}+\frac{\varphi}{R}\right),\quad \gamma_{zx}=0,\quad \gamma_{yz}=\left(\frac{\partial w}{\partial y}-\varphi\right)-x\left(\frac{\varphi}{R}+\frac{\partial \phi}{\partial y}\right) \tag{5}$$

The transverse shearing force q (Timoshenko, 1955), bending moment m and twist moment τ of the beam about these principal axes (Fig. 3b) are

$$q=\kappa\iint G\gamma_{zy}\,dA=\kappa GA\left(\frac{\partial w}{\partial y}-\varphi\right)=\kappa GA\left(\frac{1}{R}\frac{\partial w}{\partial \theta}-\varphi\right) \tag{6a}$$

$$m=\iint E\varepsilon_{yy}z\,dA=\frac{EI}{R}\left(\phi-\frac{\partial \varphi}{\partial \theta}\right) \tag{6b}$$

$$\tau=\iint G(z\gamma_{xy}-x\gamma_{yz})\,dA=C\left(\frac{\varphi}{R}+\frac{\partial \varphi}{\partial y}\right)=\frac{C}{R}\left(\varphi+\frac{\partial \phi}{\partial \theta}\right) \tag{6c}$$

in which $C=\kappa_1 Gah^3$ and κ_1 denotes the torsion coefficient (Timoshenko and Goodier 1970). The equations of motion of the entire beam, as obtained from the Hamilton's principle, are

$$-\frac{1}{R}\frac{\partial q}{\partial \theta}+\rho A\frac{\partial^2 w}{\partial t^2}=f(\theta,t),\quad q-\frac{1}{R}\frac{\partial m}{\partial \theta}-\frac{\tau}{R}=\rho I\frac{\partial^2 \varphi}{\partial t^2} \tag{7a, b}$$

$$\frac{1}{R}\frac{\partial \tau}{\partial \theta}-\frac{m}{R}=\rho J\frac{\partial^2 \phi}{\partial t^2},\quad \theta=0\sim n\alpha \tag{7c}$$

Eqs. (7a)-(7c) resemble to those obtained by Rao (1971).

The transverse deflection, bending slope, twist angle, transverse shearing force, bending moment and twist moment of the ith span are denoted respectively as w_i, φ_i, ϕ_i, q_i, m_i and τ_i which are

$$(w_i,\varphi_i,\phi_i,q_i,m_i,\tau_i)(\theta,t)=(w,\varphi,\phi,q,m,\tau)[\theta+(i-1)\alpha,t],\quad 0\le\theta\le\alpha \tag{8}$$

The displacement conditions at both ends of the span are

$$w_i(0,t)=w_i(\alpha,t)=0, \quad \phi_i(0,t)=\phi_i(\alpha,t)=0 \tag{9}$$

The bending slope continuity and zero moment at the ith support between two adjacent spans are

$$\varphi_{i-1}(\alpha,t)=\varphi_i(0,t), \quad m_{i-1}(\alpha,t)+m_i(0,t)=0 \tag{10}$$

Furthermore, the boundary conditions at both ends of the entire beam are

$$\begin{gathered} w_1(0,t)=w_n(\alpha,t)=0, \quad \phi_1(0,t)=\phi_n(\alpha,t)=0 \\ m_1(0,t)=m_n(\alpha,t)=0 \end{gathered} \tag{11}$$

3. Modal frequency

To calculate the modal frequencies of the curved beam, the transverse deflection w, bending slope φ, twist angle ϕ, transverse shearing force q, bending moment m and twist moment τ of the entire structure are expressed as

$$(\mathrm{w}\ \varphi\ \phi\ q\ m\ \tau)(\theta,t)=(W\ \Psi\ \Phi\ Q\ M\ T)(\theta)\sin(\omega t). \tag{12}$$

in which ω denotes the circular frequency. Substituting Eq. (12) into Eqs. (7a)-(7c), then omitting the term $f(\theta, t)$ yields

$$-\frac{1}{R}\frac{dQ}{d\theta}=\rho A\,\omega^2 W, \quad -Q+\frac{1}{R}\frac{dM}{d\theta}+\frac{T}{R}=\rho\omega^2 I\,\Psi \tag{13a, b}$$

$$-\frac{1}{R}\frac{dT}{d\theta}+\frac{M}{R}=\rho\omega^2 J\,\Phi \tag{13c}$$

in which

$$Q=\kappa GA\left(\frac{1}{R}\frac{dW}{d\theta}-\Psi\right), \quad M=\frac{EI}{R}\left(\Phi-\frac{d\Psi}{d\theta}\right), \quad T=\frac{C}{R}\left(\Psi+\frac{d\Phi}{d\theta}\right) \tag{14a, b, c}$$

Substituting Q of Eq. (14a) into Eq. (13a) and arranging the result yield the form

$$\frac{d\Psi}{d\theta}=\frac{1}{\kappa GR}\left(\rho\omega^2R^2+\kappa G\frac{d^2}{d\theta^2}\right)W \tag{15}$$

Substituting Q, M and T of Eqs. (14a, b, c) into Eq. (13b) and solving Φ in terms of W and Ψ yield

$$\frac{d\Phi}{d\theta}=\frac{1}{EI+C}\left\{\kappa GAR\frac{dW}{d\theta}-\left(\kappa GAR^2+C-\rho\omega^2R^2I-EI\frac{d^2}{d\theta^2}\right)\Psi\right\} \tag{16}$$

Differentiating Eq. (16) with respect to θ and substituting Eq. (15) into the result yield

$$\begin{aligned}\frac{d^2\Phi}{d\theta^2}=\frac{1}{\kappa GR(EI+C)}\Bigg\{&\kappa GEI\frac{d^4}{d\theta^4}+[\rho\omega^2R^2EI+\kappa G(\rho\omega^2R^2I-C)]\frac{d^2}{d\theta^2}\\&+\rho\omega^2R^2(\rho\omega^2R^2I-C-\kappa GAR^2)\Bigg\}W.\end{aligned} \tag{17}$$

Substituting M and T of Eqs. (14b, c) into Eq. (13c) and differentiating the result twice with

respect to θ yield

$$(C+EI)\frac{d^2}{d\theta^2}\left(\frac{d\Psi}{d\theta}\right)+\left(C\frac{d^2}{d\theta^2}-EI+\rho\omega^2R^2J\right)\frac{d^2\Phi}{d\theta^2}=0 \tag{18}$$

Substituting Eqs. (15) and (17) into Eq. (18) yields

$$\frac{d^6W}{d\theta^6}+c_1(R,\omega)\frac{d^4W}{d\theta^4}+c_2(R,\omega)\frac{d^2W}{d\theta^2}+c_3(R,\omega)W=0 \tag{19a}$$

where

$$c_1(R,\omega)=2+\rho R^2\omega^2\left(\frac{J}{C}+\frac{1}{E}+\frac{1}{\kappa G}\right)$$

$$c_2(R,\omega)=1-\rho R^2\omega^2\left(\frac{I}{C}+\frac{J}{EI}-\frac{2}{\kappa G}+\frac{AR^2}{EI}\right)+\rho^2R^4\omega^4\left(\frac{J}{\kappa GC}+\frac{1}{\kappa GE}+\frac{J}{CE}\right)$$

$$c_3(R,\omega)=\rho R^2\omega^2\left(\frac{1}{\kappa G}+\frac{AR^2}{C}\right)-\rho^2R^4\omega^4\left(\frac{I}{\kappa GC}+\frac{J}{\kappa GEI}+\frac{AR^2J}{CEI}\right)+\frac{\rho^3R^6\omega^6J}{\kappa GEC}$$

Similarly, two following equations can be obtained

$$\left\{\frac{d^6}{d\theta^6}+c_1(R,\omega)\frac{d^4}{d\theta^4}+c_2(R,\omega)\frac{d^2}{d\theta^2}+c_3(R,\omega)\right\}(\Phi,\Psi)=(0,0) \tag{19b, c}$$

The solutions for W, Φ and Ψ of the jth span to satisfy Eqs. (19a)-(19c) and Eqs. (15)-(17) are

$$W_j(\theta)=\{D_1(\theta)\}\chi_j,\quad \Psi_j(\theta)=\{D_2(\theta)\}\chi_j,\quad \Phi_j(\theta)=\{D_3(\theta)\}\chi_j \tag{20a, b, c}$$

where χ_j is a 6 by 1 column vector, the 1 by 6 row vector $\{D_1(\theta)\}$ is listed in Appendix, and two 1 by 6 row vectors $\{D_2(\theta)\}$ and $\{D_3(\theta)\}$ are

$$\{D_2(\theta)\}=\frac{1}{\kappa GR}\left(\rho\omega^2R^2\int\{D_1(\theta)\}\,d\theta+\kappa G\frac{d}{d\theta}\{D_1(\theta)\}\right)$$

$$\{D_3(\theta)\}=\frac{1}{EI+C}\left(\kappa GAR\{D_1(\theta)\}-(\kappa GAR^2+C-\rho\omega^2R^2I)\int\{D_2(\theta)\}\,d\theta+EI\frac{d}{d\theta}\{D_2(\theta)\}\right)$$

The corresponding transverse shear force Q_j, moment M_j and torque T_j are

$$Q_j(\theta)=\kappa GA\left(\frac{1}{R}\frac{d}{d\theta}\{D_1(\theta)\}-\{D_2(\theta)\}\right)\chi_j \tag{20d}$$

$$M_j(\theta)=\frac{EI}{R}\left(\{D_3(\theta)\}-\frac{d}{d\theta}\{D_2(\theta)\}\right)\chi_j \tag{20e}$$

$$T_j(\theta)=\frac{C}{R}\left(\{D_2(\theta)\}+\frac{d}{d\theta}\{D_3(\theta)\}\right)\chi_j \tag{20f}$$

Arranging Eqs. (20a)-(20f) into the vector form of

$$\{W\ \Phi Q\ T\ \Psi M\}_j^T(\theta)=[S(\theta)]\chi_j, \tag{21}$$

from which the constant vector χ_j can be solved in terms of $\{W\ \Phi Q\ T\ \Psi M\}_j^T(0)$ as

$$\chi_j=[S(0)]^{-1}\{W\ \Phi Q\ T\ \Psi M\}_j^T(0) \tag{22}$$

Therefore, the response relations at both ends of the span are

$$\{W\ \Phi Q\ T\ \Psi M\}_j^T(\alpha)=[u_1\,u_2\,u_3\,u_4\,u_5\,u_6]\{W\ \Phi Q\ T\ \Psi M\}_j^T(0) \tag{23}$$

in which u_i is the ith column vector of the following matrix

$$[u_1\,u_2\,u_3\,u_4\,u_5\,u_6]=[S(\alpha)]\,[S(0)]^{-1}$$

By adopting the condition of both twist angle and transverse displacement being zeros at θ=0, Eq. (23) will be reduced to the form

$$\{W\ \Phi Q\ T\ \Psi M\}_j^T(\alpha)=[u_3\,u_4\,u_5\,u_6]\{Q\ T\ \Psi M\}_j^T(0) \tag{24}$$

which can be expressed as

$$\{W\ \Phi Q\ T\ \Psi M\}_j^T(\alpha)=\begin{bmatrix}U_{11}\ U_{12}\\ U_{21}\ U_{22}\\ U_{31}\ U_{32}\end{bmatrix}\{Q\ T\ \Psi M\}_j^T(0) \tag{25}$$

or

$$\{W\ \Phi\}_j^T(\alpha)=[U_{11}]\{Q\ T\}_j^T(0)+[U_{12}]\{\Psi M\}_j^T(0) \tag{26a}$$

$$\{Q\ T\}_j^T(\alpha)=[U_{21}]\{Q\ T\}_j^T(0)+[U_{22}]\{\Psi M\}_j^T(0) \tag{26b}$$

$$\{\Psi M\}_j^T(\alpha)=[U_{31}]\{Q\ T\}_j^T(0)+[U_{32}]\{\Psi M\}_j^T(0) \tag{26c}$$

where $[U_{ij}]$ represents a 2 by 2 matrix. Further, the condition of both twist angle and transverse displacement being zeros at $\theta=\alpha$ implies that Eq. (26a) can be written as the form

$$\{Q\ T\}_j^T(0)=-[U_{11}]^{-1}[U_{12}]\{\Psi M\}_j^T(0) \tag{27}$$

which indicates that the transverse shear force and torque are related with the bending slope and moment at the end θ=0. Substituting Eq. (27) into Eq. (26c) yields

$$\{\Psi M\}_j^T(\alpha)=[N]\{\Psi M\}_j^T(0) \tag{28}$$

where

$$[N]=[U_{32}]-[U_{31}]\,[U_{11}]^{-1}\,[U_{12}]$$

Employing the conditions of bending slope continuity and moment balance of two adjacent spans at the jth support into Eq. (28) yields

$$\{\Psi M\}_{j+1}^T(0)=[Z]\{\Psi M\}_j^T(0) \tag{29}$$

where the transfer matrix $[Z]$ is

$$[Z]=\begin{bmatrix}1 & 0\\ 0 & -1\end{bmatrix}[N]$$

The ith modal frequency ω_i and the corresponding set of mode shape functions $\{W\ \Phi\ Q\ T\ \Psi\ M\}^{(i)}(\theta)$, $0\le\theta\le n\alpha$, of the entire beam can be obtained by performing calculations similar to that described by Wang and Lin (1997).

4. Orthogonality

The ith modal frequency and its corresponding set of mode shape functions satisfy the following equations

$$-\frac{1}{R}\frac{dQ^{(i)}}{d\theta}=\rho A\,\omega_i^2 W^{(i)},\quad -Q^{(i)}+\frac{1}{R}\frac{dM^{(i)}}{d\theta}+\frac{T^{(i)}}{R}=\rho I\,\omega_i^2\Psi^{(i)} \tag{30a, b}$$

$$-\frac{1}{R}\frac{dT^{(i)}}{d\theta}+\frac{M^{(i)}}{R}=\rho J\,\omega_i^2\Phi^{(i)} \tag{30c}$$

Multiplying Eq. (30a) by $W^{(j)}$, Eq. (30b) by $\Psi^{(j)}$ and Eq. (30c) by $\Phi^{(j)}$, respectively, and integrating their summation from θ=0 to $\theta=n\alpha$ yields

$$\omega_i^2\int_0^{n\alpha}\rho(AW^{(i)}W^{(j)}+I\Psi^{(i)}\Psi^{(j)}+J\Phi^{(i)}\Phi^{(j)})\,d\theta$$
$$=\int_0^{n\alpha}\left(\frac{Q^{(i)}Q^{(j)}}{\kappa GA}+\frac{T^{(i)}T^{(j)}}{C}+\frac{M^{(i)}M^{(j)}}{EI}\right)d\theta \tag{31}$$

Similarly, the following equation is obtained for the jth modal frequency and its corresponding set of mode shape functions

$$\omega_j^2\int_0^{n\alpha}\rho(AW^{(i)}W^{(j)}+I\Psi^{(i)}\Psi^{(j)}+J\Phi^{(i)}\Phi^{(j)})\,d\theta$$
$$=\int_0^{n\alpha}\left(\frac{Q^{(i)}Q^{(j)}}{\kappa GA}+\frac{T^{(i)}T^{(j)}}{C}+\frac{M^{(i)}M^{(j)}}{EI}\right)d\theta \tag{32}$$

Eqs. (31) and (32) imply that two distinct sets of mode shape functions are orthogonal , i.e.,

$$\int_0^{n\alpha}\rho(AW^{(i)}W^{(j)}+I\Psi^{(i)}\Psi^{(j)}+J\Phi^{(i)}\Phi^{(j)})\,d\theta=0,\qquad i\neq j \tag{33a}$$

$$\int_0^{n\alpha}\left(\frac{Q^{(i)}Q^{(j)}}{\kappa GA}+\frac{T^{(i)}T^{(j)}}{C}+\frac{M^{(i)}M^{(j)}}{EI}\right)d\theta=0,\qquad i\neq j \tag{33b}$$

or

$$\int_0^{n\alpha}\left\{\frac{W^{(j)}}{R}\frac{dQ^{(i)}}{d\theta}+\Psi^{(j)}\left(-Q^{(j)}+\frac{1}{R}\frac{dM^{(i)}}{d\theta}+\frac{T^{(i)}}{R}\right)+\frac{\Phi^{(j)}}{R}\left(-\frac{dT^{(i)}}{d\theta}+M^{(i)}\right)\right\}d\theta=0$$

for $i\neq j$. (33c)

5. Forced vibration

While examining the forced vibration, the responses of the curved beam can be expanded into the forms of mode superposition as

$$(\mathrm{w},\ \varphi,\ \phi)(\theta, t)=\sum_{i=1} b_i(t)(W^{(i)},\ \Psi^{(i)},\ \Phi^{(i)})(\theta) \tag{34a}$$

$$(q, m, \tau)(\theta, t)=\sum_{i=1} b_i(t)(Q^{(i)}, M^{(i)}, T^{(i)})(\theta) \tag{34b}$$

in which $b_i(t)$ denotes the ith modal amplitude. By performing calculations similar to that described by Wang and Lin (1997), the governing equation of $b_i(t)$ is obtained as

$$\frac{d^2 b_i}{dt^2}+\omega_i^2 b_i=g_i(t) \tag{35}$$

in which the ith modal excitation $g_i(t)$ is

$$g_i(t)=R\int_0^{n\alpha} f(\theta, t)\, W^{(i)} d\theta / D_i \tag{36}$$

where the ith modal mass D_i is

$$D_i=R\int_0^{n\alpha} \rho(AW^{(i)}W^{(i)}+I\,\Psi^{(i)}\Psi^{(i)}+J\,\Phi^{(i)}\Phi^{(i)})\, d\theta \tag{37}$$

6. Moving loads

Two types of loads moving at a constant velocity v on the multi-span curved beam are considered in this section.

6.1. Moving concentrated load

A concentrated load of magnitude of F_0 moving at a constant velocity v on the curved beam is displayed in Fig. 4. The form of the load is

$$f(\theta, t)=\begin{cases} F_0(\theta-vt/R) & 0\le t\le nT \\ 0 & nT\le t \end{cases} \tag{38}$$

where $nT(=nR\alpha/v)$ denotes the duration of load acting on the beam. The respective histories of the ith modal excitation $g_i(t)$, amplitude $b_i(t)$ and velocity $b_i(t)$ of the curved beam can be obtained as those forms described by Wang and Lin (1997).

6.2. Moving uniformly distributed load

The curved beam subjected to a uniformly distributed load f_0 with a constant velocity v is depicted in Fig. 5. The equation of the load is

$$f(\theta, t)=f_0\{H[\theta-(vt-d)/R]\}-H(\theta-vt/R)\} \tag{39}$$

in which H represents the unit step function and $d(<R\alpha)$ is the distributed length. The respective

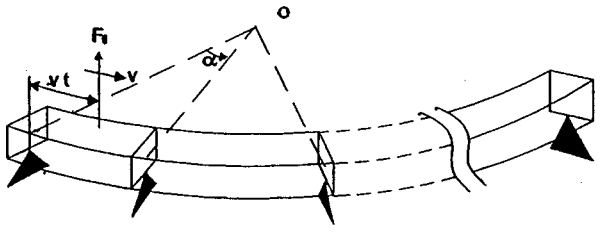

Fig. 4 A concentrated load moves on the curved beam

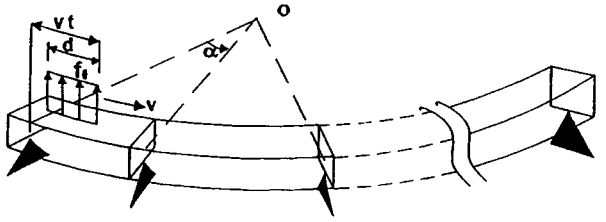

Fig. 5 A uniformly distributed load moves on the curved beam

histories of the ith modal excitation $g_i(t)$, amplitude $b_i(t)$ and velocity $b_i(t)$ of the curved beam can be also obtained as those forms described by Wang and Lin (1997).

7. Illustrative examples and discussion

In this section, the properties of beam are E=30 Gpa, ρ=2300 kg/m^3, μ=0.2, κ=0.833, a=10 m, h=1 m and κ_1=0.312. Both length and mass of the curved beam increase as α increases. Therefore, results listed in Table 1 show that the fundamental four modal frequencies of a three-span curved beam (R=100 m) decrease as α increases. Table 2 lists the comparisons of span number effect on the fundamental four modal frequencies of a curved beam (R=100 m, α=30°). All curved beam have the same first mode shape function. Therefore, the first modal frequency is independent on the span number. The second modal frequency of a one-span beam is the (j+1)th modal frequency of a j-span beam.

Table 3 compares four one-span length effects on the lowest three modal frequencies of a curved beam with total length 157.08 m. Results of the Table indicate that the smaller length of a span implies a larger modal frequencies of the beam. Table 4 compares five radius of curvature R effects on the fundamental four modal frequencies of a three-span beam with a total length of 50 m. The larger R of beam means the less coupling effect between bending moment and twist. Therefore, the modal frequencies of a straight Timoshenko beam are the upper bound of those corresponding modes of a curved beam. The above table reveals that the more coupling of bending and twist cause the less modal frequencies of beam.

Results obtained by the modal analysis method converge rather fast. It is sufficient to employ the first sixteen modal frequencies and their corresponding sets of mode shape functions of the beam in the study of forced vibration of the structure induced by moving loads. The magnitude of F_0=50 kN is considered in this section.

The following parameters are defined to illustrate the numerical results: velocity of the bending wave of the first mode $v_c=\omega_1 L/\pi$; maximum deflection of the beams during the motion of load,

Table 1 Comparisons of α (degree) effects on the fundamental four modal frequencies (rad/s) of a three-span curved beam (R=100 m)

α	ω_1	ω_2	ω_3	ω_4
20	8.28	10.67	15.63	33.42
30	3.61	4.68	6.91	14.82
50	1.22	1.62	2.44	5.26

Table 2 The span number effects on the comparisons of the fundamental four modal frequencies (rad/s) of a curved beam (R=100 m, α=30°)

span	ω_1	ω_2	ω_3	ω_4
1	3.61	14.82	33.42	59.28
2	3.61	5.75	14.82	18.79
3	3.61	4.69	6.81	14.82
4	3.61	4.25	5.75	7.43

Table 3 The one-span length L (m) effects on the comparisons of the fundamental three modal frequencies (rad/s) of a curved beam (R= 100 m) with total length 157.08 m

L	ω_1	ω_2	ω_3
157.08	0.29	1.53	3.61
78.54	1.53	2.50	6.52
52.36	3.61	4.69	6.91
39.27	6.52	7.63	10.29

Table 4 The radius of curvature R (m) effects on the comparisons the fundamental four modal frequencies (rad/s) of a three-span curved beam with total length 50 m

R	ω_1	ω_2	ω_3	ω_4
50	3.57	4.81	7.31	15.80
100	3.93	5.15	7.59	16.24
400	4.10	5.26	7.68	16.41
800	4.11	5.27	7.69	16.42
∞	4.11	5.27	7.69	16.42

w_{max}; maximum bending slope of the beams during the motion of load, φ_{max}; maximum twist angle of the beams during the motion of load, ϕ_{max}; maximum transverse shear force of the beams during the motion of load, q_{max}; maximum bending moment of the beams during the motion of load, m_{max}; maximum torque of the beams during the motion of load, τ_{max}.

The comparisons of two different effects of velocity on the histories of deflection, bending

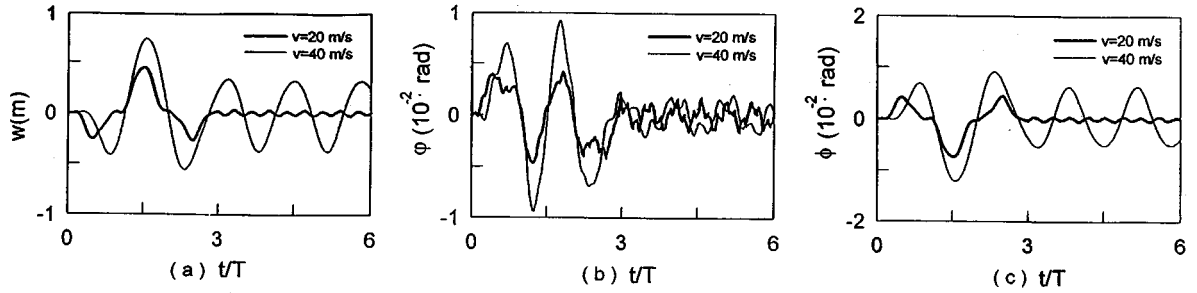

Fig. 6 Comparisons of two velocity effects of a moving concentrated load on (a) the deflection history, (b) the bending slope history and (c) the twist angle history of the mid-point of the second span of a three-span curved beam (R=100 m, α=30°)

slope and twist angle at the mid-point of the second span of a three-span curved beam (R=100 m, α=30°) induced by a concentrated moving load are displayed in Figs. 6(a)-(c), respectively. These results show that a faster speed of the moving load causes a larger deflection, a larger bending slope and a larger twist angle of the beam. A less speed ($< v_c$) of the moving load results in a longer duration of forced vibration of the beam. These maximum values, therefore, appear during the load moving on the beam at a subcritical velocity.

A three-span curved beam (R=100 m, α=30°) taken is an example to examine the effect of two types of loads on the responses of structure. A concentrated load and a uniformly distributed load (d=10 m) are considered. Further, these loads have the same magnitude of 50 kN. Comparisons of these loads on the $w_{max} - v$ distribution, the $\varphi_{max} - v$ distribution and the $\phi_{max} - v$ distribution of the curved beam are displayed in Figs. 7(a)-(c), respectively. The corresponding $q_{max} - v$ distribution, $m_{max} - v$ distribution and $\tau_{max} - v$ distribution of the curved beam are depicted in Figs. 8(a)-(c), respectively. These results in Figs. 7(a)-8(c) indicate that the concentrated load induces the absolute maximum responses among these loads. Therefore, only the effects of a moving concentrated load on the dynamic responses of curved beams are considered in the following discussions.

The reaction moments are zeros at the first hinge and the fourth hinge of a three-span beam (R= 100 m, α=30°). Consequently, the maximum deflection always appears at the mid-point of either the first span or the third span. Further, the maximum bending slope always occurs at the hinge supports. The non-twisting supports cause that the maximum twist angle always happens at the mid-

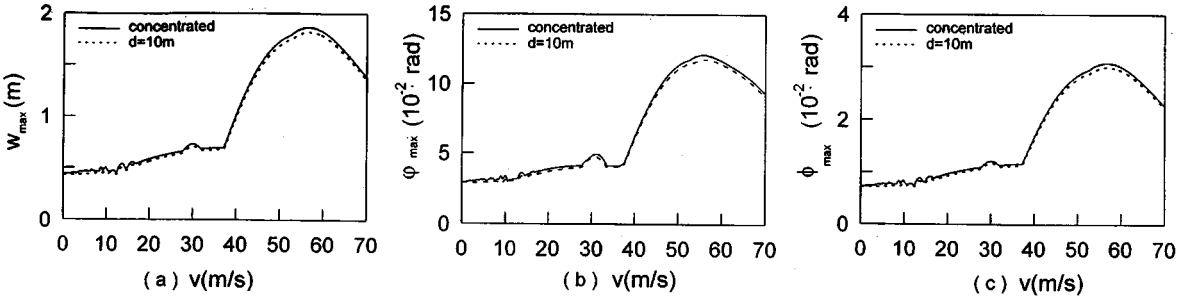

Fig. 7 Comparisons of load types on: (a) $w_{max} - v$, (b) $\varphi_{max} - v$ and (c) $\phi_{max} - v$ distributions of a three-span curved beam (R=100 m, α=30°)

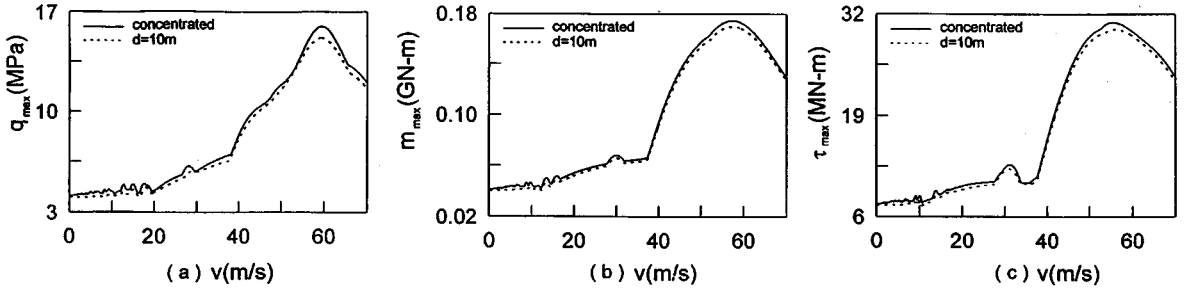

Fig. 8 Comparisons of load types on: (a) $q_{max}-v$, (b) $m_{max}-v$ and (c) $\tau_{max}-v$ distributions of a three-span curved beam (R=100 m, α=30°)

point of one span. The maximum transverse shear force of the beam appears at either the second hinge or the third hinge where the deflection is zero. The maximum moment occurs at the mid-point of either the first span or the third span of the beam. The maximum torque appears at the fourth non-twisting support where the twist angle is zero.

The effects of span number on the $w_{max}-v$ distribution, the $\varphi_{max}-v$ distribution and the $\phi_{max}-v$ distribution of a multi-span curved beam (R=100 m, α=30°) are displayed in Figs. 9(a)-(c), respectively. The moving load can be regarded as a quasi-static load within the velocity range $0\leq v\leq 20$ m/s. The reactions of transverse shear force, bending moment and torque at each rigid, hinge and non-twisting support produce a negative effect on the transverse deflection, bending slope and twist angle of a curved beam. Therefore, the more span number implies the less responses of curved beam within the velocity range $0\leq v\leq 20$ m/s. A rapidly traveling load induces a disturbance propagation in a periodically curved beam. The disturbance contains free waves and non-propagating parts, which decay spatially. Consequently, the free waves on the vibration of multi-span curved beam are more significant as the span number increases. The first modal frequency and its corresponding set of mode shape functions dominate the vibration of beam. The first mode of beam is a bending mode. The results in Figs. 9(a)-(c) demonstrate that the higher span number implies the more absolute maximum responses constrained within the neighborhood of the phase velocity of bending wave of the first mode.

The comparisons of two different L effects of a span length on the $w_{max}-v$ distribution, the $\varphi_{max}-v$ distribution and the $\phi_{max}-v$ distribution of a curved beam (R=100 m) with total length 157.08 m are displayed in Figs. 10(a)-(c), respectively. The less length of a span suggests that the curved

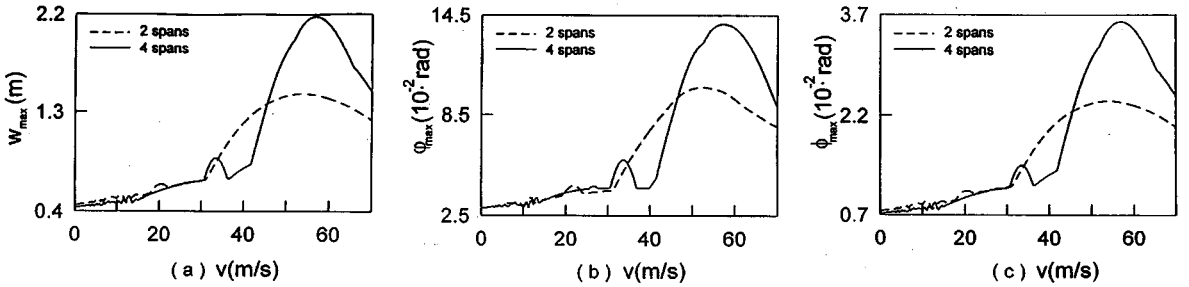

Fig. 9 Span number effect on: (a) $w_{max}-v$, (b) $\varphi_{max}-v$ and (c) $\phi_{max}-v$ distributions of a multi-span curved beam (R=100 m, α=30°) due to a concentrated load

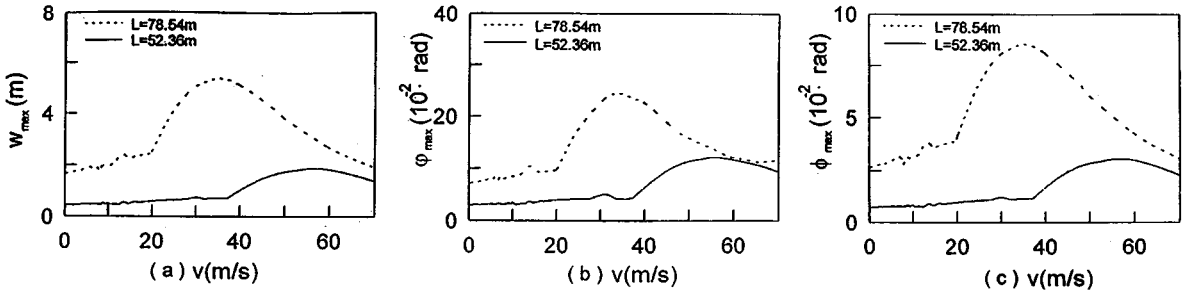

Fig. 10 Comparisons of one-span length (L) effect on: (a) $w_{max}-v$, (b) $\varphi_{max}-v$ and (c) $\phi_{max}-v$ distributions of a curved beam (R=100 m) with total length 157.08 m due to a concentrated load

beam has more support number. Therefore, the less length of a span implies the less responses of the curved beam.

8. Conclusions

This paper presents the derivation of equations of motion of a multi-span curved beam in detail. Based on the present modal analysis for the vibration of multi-span curved beams, the following conclusions can be made: (1) the first modal frequency is independent on the span number; (2) the larger the radius of curved beam causes the less coupling effect between the bending and twist; (3) the responses of a multi-span curved beam caused by a constant-velocity moving load are greater than those by the load in a static situation; (4) a critical velocity exists at which the responses of the curved beam become absolutely large; (5) the lowest bending wave velocity in the curved beam is the upper bound of the critical velocity of the beam; and (6) higher span numbers result in higher absolute responses and critical velocity.

Acknowledgements

The authors would like to thank the National Science Council, R.O.C. for financial support of this manuscript under Contract No. 87-2212-E006-035.

References

El-Amin, F.M. and Kasem, M.A. (1978), "Higher-order horizontally-curved beam finite element including warping for steel bridges", *Int. J. Numer. Methods Eng., l.* **12**, 159-167.

Lebeck, A.O. and Knowlton, J.S. (1985), "A finite element for the three-dimensional deformation of a circular ring", *Int. J. Numer. Methods Eng.*, **21**, 421-435.

Rao, S.S. (1971), "Effects of transverse shear and rotatory inertia on the coupled twist-bending vibrations of circular rings", *J. Sound. Vibra.*, **16**(4), 551-566.

Silva, Julio M.M. and Urgueira, Antonio P.V. (1988), "Out-of-plane dynamic response of curved beams-an analytical model", *Int. J. Solid. Struct.*, **24**(3), 271-284.

Timoshenko, S.P. and Young, D.H. (1955), *Vibration Problems in Engineering*, Van Nostrand Reinhold Co., New York, N. Y.

Timoshenko, S.P. and Goodier, J.N. (1970), *Theory of Elasticity*, McGRaw-Hill Co., New York, N. Y.

Volterra, E. and Gaines, J.H. (1971), *Advanced Strength of Materials*, Prentice-Hall Inc., Englewood Cliffs, N. J.

Wang, R.T. and Lin, J.S. (1997), "Vibration of multispan frames due to moving loads", *J. CSME.*, **18**(2), 151-162.

Wang, T.M., Nettleton, R.H. and Keita, B. (1980), "Natural frequencies for out-of-plane vibrations of continuous curved beams", *J. Sound. Vibra.*, **68**(3), 427-436.

Wang, T.M., Laskey, A.J. and Ahmad, M.F. (1984), "Natural frequencies for out-of-plane vibrations of continuous curved beams considering shear and rotatory inertia", *Int. J. Solid. Struct.*, **20**(3), 257-265.

Yang, Y.B. and Kuo, S.R. (1986), "Static stability of curved thin-walled beams", *Journal of Engineering Mechanics*, **12**(8), 821-841.

Appendix: list of the vector function

The vector function $\{D(\theta)\}$ depends on the roots $\lambda_i(i=1, 2, 3)$ of the equation

$$\lambda_i^6 + c_1(R, \omega)\lambda_i^4 + c_1(R, \omega)\lambda_i^2 + c_1(R, \omega) = 0 \tag{a}$$

There are six kinds of $\{D(\theta)\}$:

1) $\lambda_1 < \lambda_2 < \lambda_3 < 0$

$$\{D(\theta)\} = \{\cos(\beta_1\theta)\ \sin(\beta_1\theta)\ \cos(\beta_2\theta)\ \sin(\beta_2\theta)\ \cos(\beta_3\theta)\ \sin(\beta_3\theta)\} \tag{b}$$

where $\beta_i = \sqrt{|\lambda_i|}$, $i = 1\sim3$.

2) $\lambda_1 < \lambda_2 < 0 < \lambda_3$

$$\{D(\theta)\} = \{\cos(\beta_1\theta)\ \sin(\beta_1\theta)\ \cos(\beta_2\theta)\ \sin(\beta_2\theta)\ \cosh(\beta_3\theta)\ \sinh(\beta_3\theta)\} \tag{c}$$

3) $\lambda_1 < 0 < \lambda_2 < \lambda_3$

$$\{D(\theta)\} = \{\cos(\beta_1\theta)\ \sin(\beta_1\theta)\ \cosh(\beta_2\theta)\ \sinh(\beta_2\theta)\ \cosh(\beta_3\theta)\ \sinh(\beta_3\theta)\} \tag{d}$$

where $\beta_i = \sqrt{|\lambda_i|}$, $i = 1\sim3$.

4) $0 < \lambda_2 < \lambda_3 < \lambda_1$

$$\{D(\theta)\} = \{\cosh(\beta_1\theta)\ \sinh(\beta_1\theta)\ \cosh(\beta_2\theta)\ \sinh(\beta_2\theta)\ \cosh(\beta_3\theta)\ \sinh(\beta_3\theta)\} \tag{e}$$

5) $\lambda_1 < 0$, two conjugate λ_2 and $\overline{\lambda}_2$

$$\begin{aligned}\{D(\theta)\} = \{&\cos(\beta_1\theta)\ \sin(\beta_1\theta)\ \cos(\mu\theta)\ \cosh(\chi\theta)\ \cos(\mu\theta)\ \sinh(\chi\theta)\\ &\sin(\mu\theta)\ \cosh(\chi\theta)\ \sin(\mu\theta)\ \sinh(\chi\theta)\}\end{aligned} \tag{f}$$

where $\mu = |\lambda_2|^{1/2}\cos(0.5\arg(\lambda_2))$ and $\chi = |\lambda_2|^{1/2}\sin(0.5\arg(\lambda_2))$

6) $\lambda_1 > 0$, two conjugate λ_2 and $\overline{\lambda}_2$

$$\begin{aligned}\{D(\theta)\} = \{&\cosh(\beta_1\theta)\ \sinh(\beta_1\theta)\ \cos(\mu\theta)\ \cosh(\chi\theta)\ \cos(\mu\theta)\ \sinh(\chi\theta)\\ &\sin(\mu\theta)\ \cosh(\chi\theta)\ \sin(\mu\theta)\ \sinh(\chi\theta)\}\end{aligned} \tag{g}$$